LOCALIZED MODES IN MICROTRAP ARRAYS
SEMESTER PROJECT

ETH ZÜRICH
TRAPPED ION QUANTUM INFORMATION GROUP

Student: Javier Naya Hernández
Supervisor: Matt Grau

Spring 2021

Contents

1 Introduction

Trapped ions are a promising platform for quantum computation and simulation. Long coherence times and high-fidelity state preparation allow for the precise manipulation of ions' internal degrees of freedom which can be used for quantum information processing purposes. The coupling of the ions' motion via the Coulomb interaction allows for the coherent operation of two-qubit gates by exploiting the joint motion of the ions.

Although the physical principles of operation of various ion trap platforms are the same, different designs have been proposed to circumvent the issues arising when trying to scale up the number of ions. For example: linear chains of ions in a micro-fabricated surface electrode trap [17], Quantum Charged Coupled Device (QCCD) architecture in which the ions are physically transported between sites to perform the desired gate operations [11], or theoretical proposals for micro-fabricated arrays of micro-penning traps with individual trapping potentials [5].

Cirac and Zoller proposed microtrap arrays in the year 2000 [1] as 2D grid of harmonic potentials with individual ions trapped in them, which would allow for the implementation of quantum gates. Since then, technological advances have allowed for the trapping and manipulation of two ions in a similar linear configuration [15], and even a triangular array [9]. The microtrap approach allows for tuning the individual trap frequencies and their separation, in turn modifying the motional eigenstates of the system at low temperatures, also know as normal modes. By precisely choosing these parameters it is possible to engineer the resulting normal modes to exhibit desirable properties, such as restricting ions to only interact with their nearest neighbors, which in turn can be used for quantum simulation purposes [12, 18, 2].

For this work we studied the normal modes of the ions in a microtrap array configuration, considering only an effective harmonic potential in three dimensions without any magnetic field. The goal is to develop an understanding the structure of these modes when scaling the number of ions, or varying parameters such as distance or microtrap frequency in the system. Additionally, we proposed alternatives for creating localized motional modes, such that only a certain number of ions have significant contribution to particular motional states. This report is split between analytical studies of specific configurations of motional modes, and the numerical simulation of such systems via the python package `ion_sim`, developed for internal use by the TIQI group .

In the second section we present the common derivation for normal modes in a 1D potential, with an example in the case of two ions. We then extend the same calculation for microtraps with different frequencies and separated by arbitrary distances. For the third section, we present three different cases where we find approximate analytical expressions for mode frequencies, and the comparison to simulation results. In the fourth section, we briefly introduce the ideas behind localized modes and present two alternatives for 5 ion localization. Finally, on the fifth section we extend the simulation to allow for two dimensional arrays and show results for simple arrays.

2 Normal Mode Calculation

2.1 N ions in 1D effective potential

The problem of the motion of ions in a classical potential is a problem easily studied in the context of classical mechanics. The ions are positively charged particles that repel each other via Coulomb interaction, and the external harmonic potential brings them close together. The detail of how the potential is achieved will not be covered here in detail, but it involves a combination of static and oscillating electric fields in what is know as a Paul trap [16].

To experimentally trap the ions, one of the directions of the potential has to be weaker (axial) than the other two (radial) [4]. This allows for the ions to form a one dimensional chain structure along the axial direction, and hence the ion-ion interactions to be studied are only one dimensional. For simplicity we will be considering ions of the same species and thus having the same mass [6].

Suppose we have N ions ordered as $x_N(t) > x_{N-1}(t) > ... > x_1(t)$, where $x_i(t)$ is the position of the ion i with respect to the center of the potential time t. Taking into account the Coulomb interaction between each ion and an effective potential we can write the total potential for this problem as:

$$V = \sum_{m=1}^{N} \frac{1}{2} m\nu^2 x_m(t)^2 + \sum_{\substack{n,m=1 \\ n>m}} \frac{Z^2 e^2}{4\pi\epsilon_0} \frac{1}{|x_n(t) - x_m(t)|} \tag{1}$$

With m being the mass of each ion, ν the effective frequency of the trap along the axial direction, Z the degree of ionization, e the electron charge and ϵ_0 the permittivity of free space. For this configurations, and ignoring any thermal fluctuations from the ions, the system will reach an equilibrium position when $(\partial V/\partial x_m)\,|_{x_m = x_m^{(0)}} = 0$, with $x_i^{(0)}$ being the equilibrium position for the ion i. The derivative is as it follows:

$$\frac{\partial V}{\partial x_i} = m\nu^2 x_i - \sum_{j=1}^{i-1} \frac{Z^2 e^2}{4\pi\epsilon_0} \frac{1}{(x_i - x_j)^2} + \sum_{j=i+1}^{N} \frac{Z^2 e^2}{4\pi\epsilon_0} \frac{1}{(x_i - x_j)^2} \tag{2}$$

Where the second term accounts for the ions with $x_j < x_i$ and the third term for $x_j > x_i$, the time dependence of the coordinates is omitted to simplify the notation. Introducing a dimensionless scale factor $u_m = x_m^{(0)}/l$ with $l^3 = (Z^2 e^2)/(4\pi\epsilon_0 m\nu^2)$ allows us to simplify the equations to:

$$u_i - \sum_{j=1}^{i-1} \frac{1}{(u_i - u_j)^2} + \sum_{j=i+1}^{N} \frac{1}{(u_i - u_j)^2} = 0 \tag{3}$$

With the index i is running from 1 to N and defining a set of N coupled non linear equations that define the ions' equilibrium positions.

As mentioned in the introduction, the motional modes of arrays of ions allow for the operation of two-qubit gates, such as the Molmer-Sorensen gate [13]. In order to perform these operations the motion of the ions has to be cooled to near ground state. We can then treat the motion of the ions as a small perturbation around the equilibrium position $x_i = x_i^0 + q_i$. We can do a series expansion up to second order of the potential defined in equation (1) expressed with the new coordinates q_i:

$$V = V|_{x=x^{(0)}} + \sum_{i=1}^{N} q_i \frac{\partial V}{\partial x_i}\Big|_{x_i = x_i^{(0)}} + \frac{1}{2} \sum_{i,j=1}^{N} q_i q_j \frac{\partial^2 V}{\partial x_j \partial x_i}\Big|_{\substack{x_i = x_i^{(0)} \\ x_j = x_j^{(0)}}} \tag{4}$$

The first term is a constant that does not affect the dynamics of the system while the second one evaluates to zero. Calculating the third term by doing a second derivative of equation (1):

$$\frac{\partial^2 V}{\partial x_j \partial x_i} = m\nu^2 \delta_{i,j} + \sum_{m=1}^{i-1} \frac{Z^2 e^2}{2\pi\epsilon_0} \frac{\delta_{i,j} - \delta_{j,m}}{(x_i - x_m)^3} - \sum_{m=i+1}^{N} \frac{Z^2 e^2}{2\pi\epsilon_0} \frac{\delta_{i,j} - \delta_{j,m}}{(x_i - x_m)^3} \tag{5}$$

$$i = j \quad \Rightarrow \quad m\nu^2 + \sum_{\substack{m=1 \\ m\neq i}}^{N} \frac{Z^2 e^2}{2\pi\epsilon_0} \frac{1}{|x_i - x_m|^3} = m\nu^2 \left(1 + 2 \sum_{\substack{m=1 \\ m\neq i}}^{N} \frac{1}{|u_i - u_m|^3} \right) \tag{6}$$

$$i \neq j \quad \Rightarrow \quad -\frac{Z^2 e^2}{2\pi\epsilon_0} \frac{1}{|x_i - x_j|^3} = m\nu^2 \left(\frac{-2}{|u_i - u_j|^3} \right) \tag{7}$$

The constants multiplying equations (6) and (7) can be factorized, so we can express $\partial V^2 / \partial x_j \partial x_i = m\nu^2 A_{i,j}$, with:

$$A_{i,i} = 1 + 2 \sum_{\substack{m=1 \\ m\neq i}}^{N} \frac{1}{|u_i - u_m|^3} \tag{8}$$

$$A_{i,j} = -\frac{2}{|u_i - u_j|^3} \tag{9}$$

Using the potential express in terms of the linearized coordinates the Lagrangian of the system is constructed as it follows:

$$\mathcal{L} = \sum_{i=1}^{N} \frac{m}{2} \dot{q_i}^2 - \frac{1}{2} m\nu^2 \sum_{i,j=1}^{N} q_i q_j A_{i,j} \tag{10}$$

The matrix $A_{i,j}$ is real and symmetric, thus it has positive eigenvalues and can be ortho-normalized. We can express it as $\mathbf{A} = \mathbf{B}\mathbf{\Lambda}\mathbf{B}^T$, where $\mathbf{B}$ is a matrix consisting of the columns of the eigenvectors of A, and $\mathbf{\Lambda}$ is the matrix with the eigenvalues of A as the diagonal entries. Inserting into the Lagrangian with vector notation gives the result:

$$\mathcal{L} = \frac{m}{2} \left[(\dot{\vec{q}})^T \dot{\vec{q}} - \nu^2 \vec{q}^T \mathbf{B}\mathbf{\Lambda}\mathbf{B}^T \vec{q} \right] \tag{11}$$

$$\mathcal{L} = \frac{m}{2} \left[(\dot{\vec{Q}})^T \dot{\vec{Q}} - \nu^2 \vec{Q}^T \mathbf{\Lambda} \vec{Q} \right] \tag{12}$$

$$\mathcal{L} = \frac{m}{2} \sum_{i=1}^{N} \left[\dot{Q}_i^2 - \nu^2 \lambda_i Q_i^2 \right] \tag{13}$$

Where we used the orthogonality of $\mathbf{B}(\mathbf{B}\mathbf{B}^T = \mathbb{1})$ and defined the normal modes $\vec{Q} = \sum_i^N \vec{b}_i q_i$, where the $\vec{b_i}$ are the eigenvectors of A.

Equation (13) can be solved by using the Euler-Lagrange equation, and results in a set of N decoupled harmonic oscillators for the normal modes $\vec{Q}$, each with a frequency $\omega_i = \nu\sqrt{\lambda_i}$.

2.1.1 Two ion case

To illustrate in more practical terms the calculation of the modes we present the solution for the case of two ions. The equilibrium position follows from (3):

$$u_1 + \frac{1}{(u_1 - u_2)^2} = 0 \tag{14}$$

$$u_2 - \frac{1}{(u_1 - u_2)^2} = 0 \tag{15}$$

The resulting solution are $u_1 = -2^{-2/3}$ and $u_2 = 2^{-2/3}$. $\mathbf{A}$ can be then calculated as:

$$\mathbf{A} = \begin{pmatrix} 2 & -1 \\ -1 & 2 \end{pmatrix} \tag{16}$$

with eigenvalues and eigenvectors:

$$\lambda_1 = 1 \;\; \vec{b}_1 = \begin{pmatrix} 1 \\ 1 \end{pmatrix} \tag{17}$$

$$\lambda_2 = 3 \;\; \vec{b}_1 = \begin{pmatrix} -1 \\ 1 \end{pmatrix} \tag{18}$$

The first eigenvector (17) is known as the *Center of Mass* (COM) mode, in which the ions oscillate with the same phase, i.e. if one moves to the right the other one does as well such that the distance between the two is conserved. The second eigenvector (18) is known as the stretch mode, where the ions oscillate with exactly opposite phase.

2.2 N ions in a 1D microtrap array

Whereas in the previous section we considered an effective potential acting on all the ions, for the microtrap array we will assume each ion having their own external harmonic potential acting on it. These microtraps will only contain one ion, which we still assume to be of the same species, and can be placed with arbitrary distance from each other. For the following calculations we will work with the coordinates $r_i(t)$ representing the distance of the i-th ion to the center of its trap. If the distance between trap i and j is $d_{i,j} = d_i - d_j$, then we can directly express r_i in terms of the previous coordinate system as $r_i = x_i - d_{1,i}$. Writing down the potential in terms of this new coordinate system:

$$V = \sum_{i=1}^{N} \frac{1}{2} m \nu_i r_i^2 + \sum_{\substack{i,j=1 \\ i \neq j}}^{N} \frac{Z^2 e^2}{4\pi\epsilon_0} \frac{1}{|r_i - r_j + d_{i,j}|} \tag{19}$$

Repeating the previous procedure to find the equilibrium positions we arrive at a very similar expression:

$$\frac{\partial V}{\partial r_i} = m\nu_i^2 r_i - \sum_{j=1}^{i-1} \frac{Z^2e^2}{4\pi\epsilon_0} \frac{1}{(r_i - r_j + d_{i,j})^2} + \sum_{j=i+1}^{N} \frac{Z^2e^2}{4\pi\epsilon_0} \frac{1}{(r_i - r_j + d_{i,j})^2} = 0 \tag{20}$$

The difference with respect to equation (3) are the different trap frequencies in each index, so we define a frequency dependant scaling $u_i = r_i^{(0)}/l_i$ with $l_i^3 = (Z^2e^2)/(4\pi\epsilon_0 m\nu_i^2)$, such that we can rewrite our system of equations as:

$$u_i - \sum_{j=1}^{i-1} \frac{1}{\left(u_i - u_j \left(\frac{\nu_i}{\nu_j}\right)^{2/3} + \frac{d_{i,j}}{l_i}\right)^2} + \sum_{j=i+1}^{N} \frac{1}{\left(u_i - u_j \left(\frac{\nu_i}{\nu_j}\right)^{2/3} + \frac{d_{i,j}}{l_i}\right)^2} = 0 \tag{21}$$

And as for the second order derivatives:

$$\frac{\partial^2 V}{\partial r_j \partial r_i} = m\nu_i^2 \delta_{i,j} + \sum_{m=1}^{i-1} \frac{Z^2e^2}{2\pi\epsilon_0} \frac{\delta_{i,j} - \delta_{j,m}}{(r_i - r_m + d_{i,j})^3} - \sum_{m=i+1}^{N} \frac{Z^2e^2}{2\pi\epsilon_0} \frac{\delta_{i,j} - \delta_{j,m}}{(r_i - r_m + d_{i,j})^3} \tag{22}$$

$$i = j \quad \Rightarrow \quad m\nu_i^2 \left(1 + 2\sum_{\substack{m=1 \\ m\neq i}}^{N} \frac{1}{|u_i - u_m(\frac{\nu_i}{\nu_m})^{\frac{2}{3}} + \frac{d_{i,m}}{l_i}|^3}\right) \tag{23}$$

$$i \neq j \quad \Rightarrow \quad m\nu_i^2 \left(\frac{-2}{|u_i - u_j(\frac{\nu_i}{\nu_j})^{\frac{2}{3}} + \frac{d_{i,j}}{l_i}|^3}\right) \tag{24}$$

We can proceed as before defining $\partial^2 V/\partial x_j \partial x_i = m\nu_i^2 A_{i,j}$, but an important difference is that, although $\partial^2 V/\partial x_j \partial x_i$ is a symmetric quantity in the indices i and j, $A_{i,j}$ is not, as seen from the following calculation:

$$\begin{aligned} \frac{1}{m\nu_i^2}\frac{\partial^2 V}{\partial r_j \partial r_i} = A_{i,j} &= \frac{-2}{|u_i - u_j(\frac{\nu_i}{\nu_j})^{\frac{2}{3}} + \frac{d_{i,j}}{l_i}|^3} = \frac{l_i^3}{l_j^3}\frac{-2}{|u_i\frac{l_i}{l_j} - u_j\frac{l_i}{l_j}(\frac{\nu_i}{\nu_j})^{\frac{2}{3}} + \frac{d_{i,j}}{l_j}|^3} \\ &= \frac{\nu_j^2}{\nu_i^2}\frac{1}{|u_j - u_i(\frac{\nu_j}{\nu_i})^{\frac{2}{3}} + \frac{d_{j,i}}{l_j}|^3} = \frac{\nu_j^2}{\nu_i^2}A_{j,i} \end{aligned} \tag{25}$$

In order to preserve the real and positive eigenvalue properties of symmetric matrices, the Lagrangian has to be written in the form:

$$\mathcal{L} = \sum_{i=1}^{N-1} \frac{m}{2}\dot{q_i}^2 - \sum_{i,j=1}^{N} \frac{m}{2} q_i q_j \frac{\partial^2 V}{\partial r_j \partial r_i} \tag{26}$$

and the solutions to the Euler-Lagrange equations will have a frequency dependence of $\omega_i = \sqrt{\lambda_i}$, where λ_i is the i-th eigenvalue of the second order derivative of the potential. That is, there will not be an explicit ν_i dependence as before.

2.2.1 Two ion case

When dealing with microtrap arrays the solution for the equilibrium positions is not as straightforward as in the standard harmonic trap. Whereas before an analytic solution could be obtained for the simple two ion case, now the system of equations requires a numerical solution:

$$u_0 + \frac{1}{\left(u_0 - u_1\left(\frac{\nu_0}{\nu_1}\right)^{\frac{2}{3}} - \frac{d}{l_0}\right)^2} = 0 \tag{27}$$

$$u_1 + \frac{1}{\left(u_1 - u_0\left(\frac{\nu_1}{\nu_0}\right)^{\frac{2}{3}} - \frac{d}{l_1}\right)^2} = 0 \tag{28}$$

The expected behavior is observed when substituting the cases $d = 0$ and $d \to \infty$, with the former recovering the known solution of the previous section, and the latter having both ions without interaction in the bottom ($u_{0,1} = 0$) of their respective potentials. In the case when one of the trap frequencies is much greater than the other one ($\nu_0 \gg \nu_1$), we have the simplified system of equations:

$$u_0 \approx 0 \tag{29}$$

$$u_1 - \frac{1}{(u_1 - \frac{d}{l_1})^2} \approx 0 \tag{30}$$

where the ion in the high frequency trap is barely affected by the presence of the one in the low frequency trap. While the latter sees the first one as a point charge sitting in the bottom of the trap.

To find the eigenstates of the system we write down the Hessian elements in the form $H_{i,j} = \partial^2 V/\partial r_j \partial r_i$:

$$H_{0,0} = \nu_0^2 \left(1 + \frac{2}{\left| u_0 - u_1 \left(\frac{\nu_0}{\nu_1} \right)^{\frac{2}{3}} - \frac{d}{l_0} \right|^3} \right) = \nu_0^2 \left(1 + 2c_{0,1} \right) \tag{31}$$

$$H_{1,1} = \nu_1^2 \left(1 + \frac{2}{\left| u_1 - u_0 \left(\frac{\nu_1}{\nu_0} \right)^{\frac{2}{3}} + \frac{d}{l_1} \right|^3} \right) = \nu_1^2 \left(1 + 2\frac{\nu_0^2}{\nu_1^2} c_{0,1} \right) \tag{32}$$

$$H_{0,1} = \frac{-2\nu_0^2}{\left| u_1 - u_0 \left(\frac{\nu_1}{\nu_0} \right)^{\frac{2}{3}} - \frac{d}{l_0} \right|^3} = -2\nu_0^2 c_{0,1} \tag{33}$$

$$H_{1,0} = \frac{-2\nu_1^2}{\left| u_0 - u_1 \left(\frac{\nu_0}{\nu_1} \right)^{\frac{2}{3}} + \frac{d}{l_1} \right|^3} = -2\nu_0^2 c_{0,1} \tag{34}$$

$$\tag{35}$$

where we introduced the variable $c_{0,1}$ which represent the mode coupling strength between the first and the second ion, and is explicitly defined as:

$$c_{0,1} = \frac{1}{\left| u_0 - u_1 \left(\frac{\nu_0}{\nu_1} \right)^{\frac{2}{3}} - \frac{d}{l_0} \right|^3} \tag{36}$$

Substituting those expressions in the known solutions for the eigenvalues of a 2x2 symmetric matrix:

$$\lambda_\pm = \frac{1}{2} \left(H_{0,0} + H_{1,1} \pm \sqrt{\left(H_{1,1} - H_{0,0} \right)^2 + 4H_{0,1}^2} \right) \tag{37}$$

$$\lambda_\pm = \frac{1}{2} \left(\nu_0^2 + \nu_1^2 \ + 4c_{0,1}\nu_0^2 \pm \sqrt{\left(\nu_1^2 - \nu_0^2 \right)^2 + 16\nu_0^4 c_{0,1}^2} \right) \tag{38}$$

For the simple case when $\nu_0 = \nu_1$ we recover the solutions:

$$\lambda_- = \nu_1^2 \tag{39}$$

$$\lambda_+ = \nu_1^2 \left(1 + 4c_{0,1} \right) \tag{40}$$

The stretch mode frequency is different compared to the result obtained in equation (18) with the standard trap potential, which has a value of $\lambda_+ = 3$. For a simulation with two calcium ions in microtraps a $\lambda_+ \sim 1/d^3$ decay is observed due to the distance dependence in $c_{0,1}$.

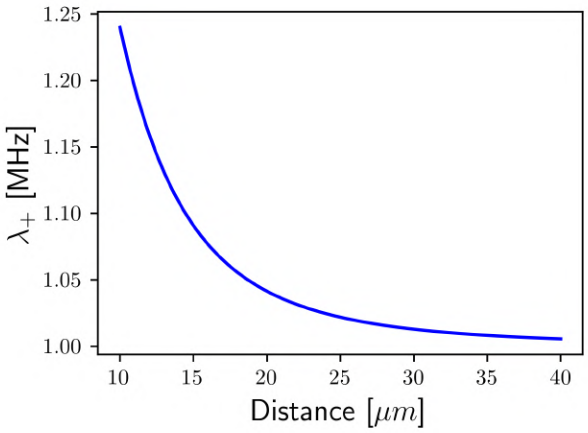

Figure 1: Values for the λ_+ eigenvalue in microtrap array with $m = 40$ amu and $\nu_1 = \nu_2 = 1$ MHz. This corresponds to the square of the stretch mode frequency

From the figure (1) we can see that for around a typical experiment of $d = 30\mu m$, we have a value of $\lambda_+ = 1.0128$, which means the difference between the stretch and COM modes is of only of $\Delta\nu = 6.4$ kHz as opposed to the $\Delta\nu = 732$ kHz difference in a standard harmonic trap with a frequency of 1 MHz. This could be problematic when applying a Molmer-Sorensen gate, due to the lower frequency spacing of the modes.

In figure (2) we can observe the behaviour of the λ_+ and λ_- eigenvalues when the ν_i frequencies are different. After a certain frequency difference between ν_1 and ν_0, the eigenvalues approach the values $\lambda_+ = \nu_1$, $\lambda_- = \nu_0$, as expected when the motion of the ions is decoupled.

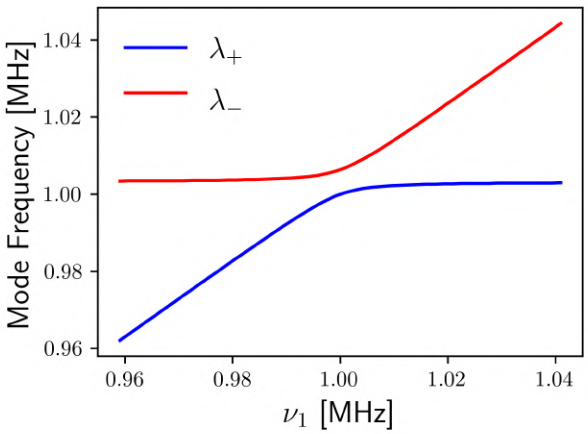

Figure 2: Values for the λ_+ and λ_+ eigenvalues in microtrap array with $m = 40$ amu $d = 30$ μm and $\nu_0 = 1$ MHz

With the eigenvalues in hand it is possible to study the structure of the normal modes, to confirm we indeed recover the expected COM and stretch mode in microtrap arrays in the case when $\nu_0 = \nu_1$

$$b_+ = C \begin{pmatrix} H_{0,1} \\ \lambda_+ - H_{0,0} \end{pmatrix} = C \begin{pmatrix} -2\nu_1^2 c_{0,1} \\ 2\nu_1^2 c_{0,1} \end{pmatrix} = \frac{1}{\sqrt{2}} \begin{pmatrix} -1 \\ 1 \end{pmatrix} \tag{41}$$

$$b_- = C \begin{pmatrix} H_{0,1} \\ \lambda_- - H_{0,0} \end{pmatrix} = C \begin{pmatrix} -2\nu_1^2 c_{0,1} \\ -2\nu_1^2 c_{0,1} \end{pmatrix} = \frac{1}{\sqrt{2}} \begin{pmatrix} 1 \\ 1 \end{pmatrix} \tag{42}$$

An important behavior in the case of the normal modes of microtrap arrays with different frequencies is the decoupling of the ions from certain normal modes. Such that in cases where the difference in frequency between the sites is greater than the exchange frequency $\Omega_{ex} = e^2/(4\pi\epsilon_0 m\omega_0 d^3)$, there are no normal modes where both ions oscillate together. This can be seen in the figure (3), where the values of the first component of the normal modes, corresponding to the contribution of the first ion to the motional mode.

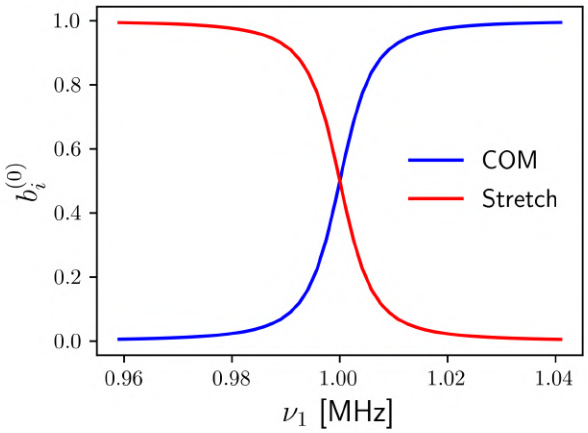

Figure 3: Contribution of the first ion to the motional modes b_+ (COM) and b_- (Stretch) in a configuration with the first trap frequency set to $\nu_0 = 1$ MHz, and $d = 30$ μm. The frequency range for ν_1 being from 1 - Ω_{ex} to 1 + Ω_{ex}

So if we wish the ions of our microtraps to interact via motional coupling, it is required that their microtrap frequency differences are on the order of around 50 kHz if dealing with typical trap frequencies of the order of 1 MHz.

2.3 Simulation

As seen from section 2.2.1, analytical solutions to even simple cases for microtrap arrays are complicated. More complex configurations require the use of numeric solutions to find the eigenvectors and frequencies corresponding. We achieved this by working with a python package created by Matthew Grau called *ion_sim* to numerically solve for ion motion in arbitrary potentials. This is done by creating a class where this potentials can be defined and built in methods that numerically calculate the normal modes and equilibrium positions via automatic differentiation package *autograd* [8], a method to efficiently calculate numerical derivatives, of the sum of the trap and the Coulomb potential.

For standard linear ion traps the potential is straightforward to calculate, defining a harmonic potential for x, y and z. In the case of the microtrap array we defined a piecewise potential, where there is either a distance defined as a input (1D case) or a set of coordinates (2D case) that will

serve as the origin for each of the microtraps. The limits beings halfway the distance to the nearest origin point (1D case), or a circle with radius halfway the distance to the nearest coordinate (2D case). Providing a list of frequencies will completely define the potentials. The code used to derive all the results in this project can be found in `https://gitlab.phys.ethz.ch/graum/ion_sim/-/blob/Javier_Project/examples/Project_Javier.ipynb`.

In figure (4) we show a standard output by the simulator. The columns of the left side of the figure represents the eigenvectors, while the rows are the contribution of each ion to each motional mode. From this figure we can recognize the COM and stretch modes as the first and second columns. On the lower side of the figure we can see a plot of the corresponding frequencies for each of the modes. The right side of the figure shows a direct comparison of the simulation and the diagonalization of the equation (22). The good match between the two gives us a good indication of the validity of the derivations done in section 2.1.

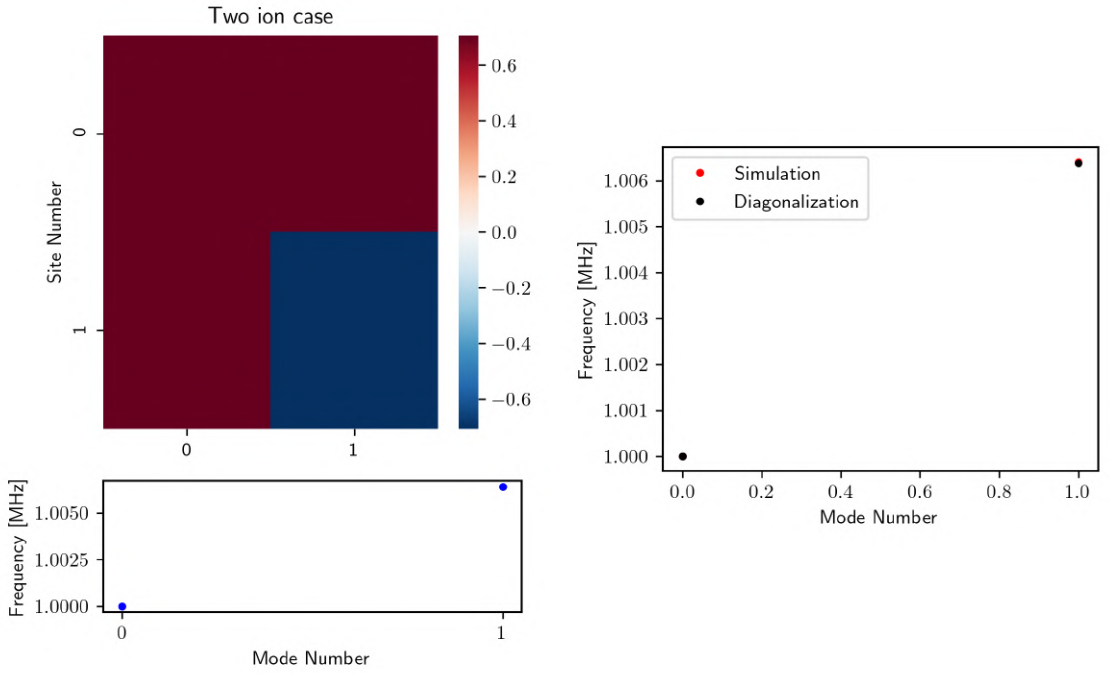

Figure 4: Left figure shows the eigenvectors and mode frequency for two ions with $m = 40$ amu, $d = 30$ μm and $\nu_0 = \nu_1 = 1$ MHz. Right figure shows the comparison of simulation with the diagonalization of the matrix defined by equation (22)

3 Analytical Approximation

To find the normal modes of an ion configuration we need to find the eigenstates and eigenvalues of a general symmetric matrix, which in general does not have a closed-form solution. Although this is not a numerically hard problem it is interesting to consider approximations on different types of arrays that reduce the problem to one with an analytical solution.

The case of a long string of ions, a long array of repeating pairs of closely spaced ions (or alternating distances), and periodic boundary conditions will be presented. To approach them we will consider only nearest-neighbor interactions for the first two cases. This is not an unreasonable assumption given that off diagonal elements decay with the inverse power law $A_{i,j}$ $1/d^3$, such that for an equally spaced array $A_{i,i+2} = A_{i,i+1}/8$.

3.1 Ion string

The solution to a long string of ions in a single trapping potential is well known and has been extensively studied numerically [6]. But in our configuration, the constant distance between traps yields a different mode structure that is more akin to the isospaced linear string studied in [7]. Although most of the features we will study have been already covered in that paper, here the contribution comes from the attempt to obtain an analytical expression for the eigenvectors and frequencies.

For the microtrap configuration we have a high radial (ω_x and ω_y) trapping potential compared to the axial direction (ω_z), equal spacing d between the ions and all traps sharing the same axial frequencies. Furthermore, we will assume the rest positions to be at the trap centers ($u_i = 0$), this approximation holds for an infinitely long chain, but even in the finite case the displacement is small enough compared to d that it doesn't significantly affect the results as can be seen in figure (5) where the ions in the edges are at most displaced by 0.4 μm.

Taking then into account only nearest-neighbour interactions, and approximating the diagonal element of the first and last ions to be the same as the rest, we can write the normal mode matrix as in a tridiagonal Toeplitz form:

$$A = \begin{pmatrix} \beta & g & & & & 0 \\ g & \beta & g & & & \\ & g & \beta & g & & \\ & & & \ddots & & \\ & & & & g & \\ 0 & & & & g & \beta \end{pmatrix} \tag{43}$$

with entries

$$\beta = \omega_z^2 \left(1 + \frac{4l^3}{d^3}\right) \tag{44}$$

$$g = -\omega_z^2 \frac{2l^3}{d^3} \tag{45}$$

The eigensystem solution to matrix of the type (43) are well know in the literature [10]. To solve for the eigenvalues of a matrix we have to find the roots of the polynomial:

$$det(A - \lambda I) = \begin{vmatrix} \frac{\beta-\lambda}{g} & 1 & & & & 0 \\ 1 & \frac{\beta-\lambda}{g} & 1 & & & \\ & 1 & \frac{\beta-\lambda}{g} & 1 & & \\ & & & & \ddots & \\ 0 & & & & & \end{vmatrix} = 0 \tag{46}$$

For a system of size N the expression in (46) can be expanded as:

$$P_n(\mu) = \mu \underbrace{\begin{vmatrix} \frac{\beta-\lambda}{g} & 1 & & & 0 \\ 1 & \frac{\beta-\lambda}{g} & 1 & & \\ & 1 & \frac{\beta-\lambda}{g} & 1 & \\ & & & \ddots & \\ 0 & & & & \end{vmatrix}}_{\text{Size N-1}} - \underbrace{\begin{vmatrix} \frac{\beta-\lambda}{g} & 1 & & & 0 \\ 1 & \frac{\beta-\lambda}{g} & 1 & & \\ & 1 & \frac{\beta-\lambda}{g} & 1 & \\ & & & \ddots & \\ 0 & & & & \end{vmatrix}}_{\text{Size N-2}} \tag{47}$$

where $\mu = \frac{\beta-\lambda}{g}$. This can be expressed as the recurrence relation, with the initial conditions:

$$P_n(\mu) = \mu P_{n-1}(\mu) - P_{n-2} \tag{48}$$

$$P_2(\mu) = \mu^2 - 1 \tag{49}$$

$$P_1(\mu) = \mu \tag{50}$$

which defines the well-known Chebyshev polynomials with zeros in $\mu_r = 2\cos(\frac{r\pi}{N+1})$, so the eigenvalues are:

$$\lambda_r = \beta - 2g\cos\left(\frac{r\pi}{N+1}\right) \tag{51}$$

$$\lambda_r = \omega_z^2\left(1 + \frac{8l^3}{d^3}\cos^2\left(\frac{r\pi}{2(N+1)}\right)\right) \tag{52}$$

with $r = 1, 2, ..., N$

The mode frequencies resulting from the solutions to the harmonic oscillator according to (26) are then:

$$\omega_r = \omega_z\sqrt{1 + \frac{8l^3}{d^3}\cos^2\left(\frac{r\pi}{2(N+1)}\right)} \tag{53}$$

The analytical expression of the eigenvectors given in [10] are of the simple form:

$$b_{r,k} = \sin\left(\frac{rk\pi}{N+1}\right) \tag{54}$$

representing the rth entry with of the kth eigenvector. Notice there is no eigenvector with all the entries having the same weight, so there is no COM mode when considering only nearest neighbor interactions.

In figure (5) we present the simulation results of a chain of 30 ions in microtrap, while in figure (6) a comparison of the results with the results in equations (53) and (54). Although the modes from the simulation and the analytical results strongly resemble each other, the former does posses a COM mode where all ions oscillate in phase. As for the eigenvalues, the approximation follows closely the frequencies obtained by simulation but having lower frequencies for higher number modes. Such shift can be attributed to only considering nearest-neighbor interactions, which lowers the value of the potential energy in the system and thus the frequency of modes where the second neighbor interaction becomes more meaningful.

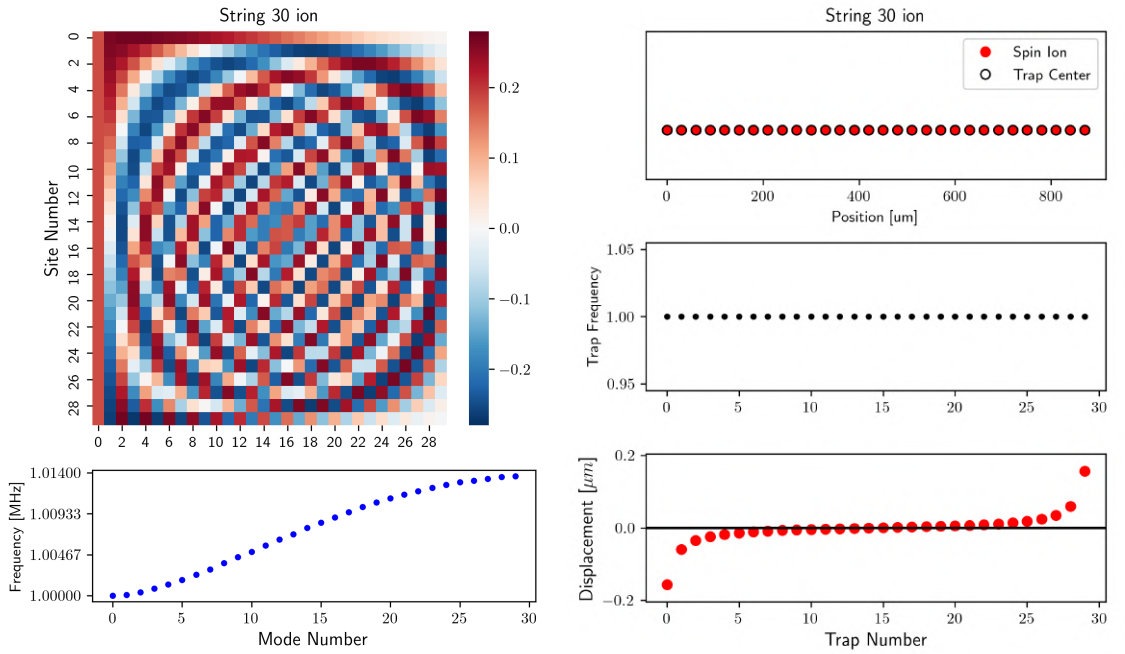

Figure 5: Simulation of 30 ions in microtraps with $m = 40$ amu, $d = 30$ μm and $\nu_i = 1$ MHz. The second figure shows the positioning of the ions, the microtrap frequencies and the displacement from the origin.

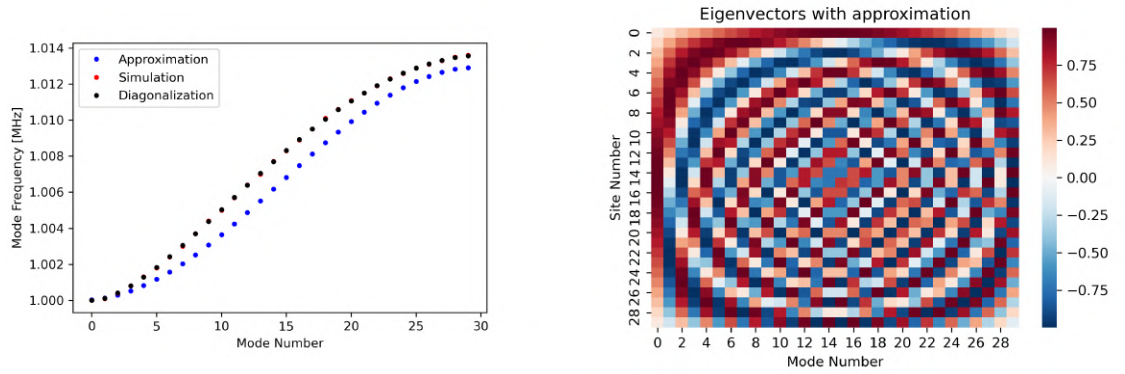

Figure 6: Left figure shows the comparison between the eigenvalues in equation (53) and the simulation with 30 ions, alongside a diagonalization of the matrix defined by (22). Right figure plots the eigenvectors in equation (54) for 30 ions.

3.2 Alternating distance

For the second case we will consider an array where the distance between each of the traps alternates after every ion. That is, the chain with groups of two ion traps close together with a distance d_1 between them, and a distance d_2 from the other nearest ion. For this problem we will also approach it using the nearest neighbor approximation, reducing the problem to the one of a 2-Toepliz matrix of the form:

$$A = \begin{pmatrix} \beta & g_1 & & & & 0 \\ g_1 & \beta & g_2 & & & \\ & g_2 & \beta & g_1 & & \\ & & & \ddots & & \\ 0 & & & & g_{1,2} & \beta \end{pmatrix} \tag{55}$$

with the second to last element being g_1 if the size N of the matrix is odd and g_2 if its even. And with:

$$\beta = \omega_z^2 \left(1 + 2l^3 \left(\frac{1}{d_1^3} + \frac{1}{d_2^3}\right)\right) \tag{56}$$

$$g_1 = -\omega_z^2 \frac{2l^3}{d_1^3} \tag{57}$$

$$g_2 = -\omega_z^2 \frac{2l^3}{d_2^3} \tag{58}$$

In order to obtain a closed expression for the eigensystem, we will assume as before that the ions rest in their equilibrium positions. Although this is is not the case even when considering an infinite array. We can justify it by observing that the ions are displaced around 0.1 micrometers at most when performing a simulation for $d_1 = 30\ \mu m$ and $d_2 = 45\ \mu m$, as seen in figure (7).

The solution for this type of system is more involved but also consists of finding a recursive relationship for the characteristic equation of the matrix (55) [3]. The results are split into the case when the size of the matrix is $N = 2m$ and $N = 2m + 1$. There exist a formula for the former, but it includes the zeros of a polynomial that, although it possesses the Chebyshev recurrence formula, the initial conditions are not Chebyshev polynomials. In case of the latter there is an explicit solution as:

$$\lambda_{r,\pm} = \beta \pm \sqrt{g_1^2 + g_2^2 + 2|g_1||g_2| \cos\left(\frac{r\pi}{m+1}\right)} \tag{59}$$

for $r = 1, 2, ..., m$, and the eigenvalue $\lambda_0 = \beta$. In the case where $g_1 = g_2$, it can be shown that the formula reduces to equation (51). The motional modes frequencies will then be:

$$\omega_{r,\pm} = \omega_z \sqrt{1 + 2l^3 \left(\frac{1}{d_1^3} + \frac{1}{d_2^3}\right) \pm 2l^3 \sqrt{\left(\frac{1}{d_1^6} + \frac{1}{d_2^6}\right) + \frac{2}{d_1^3 d_2^3} \cos\left(\frac{r\pi}{m+1}\right)}} \tag{60}$$

There is also a way to explicitly calculate the eigenvectors in terms of the Chebyshev polynomials, but their expression is much more complicated than the standard Toepliz matrix and for that reason we will obtain them by numerically diagonalizing the matrix (55).

In figure (7) can find the simulation for a case with 31 ions. The eigenvectors can be understood as a $(N-1)/2$ chain of groups of two ions oscillating as a standard ion string. In half of the modes, the two ions forming each group move in the same directions, while in the other half they mode with opposite phase and with no contribution from the last ion.

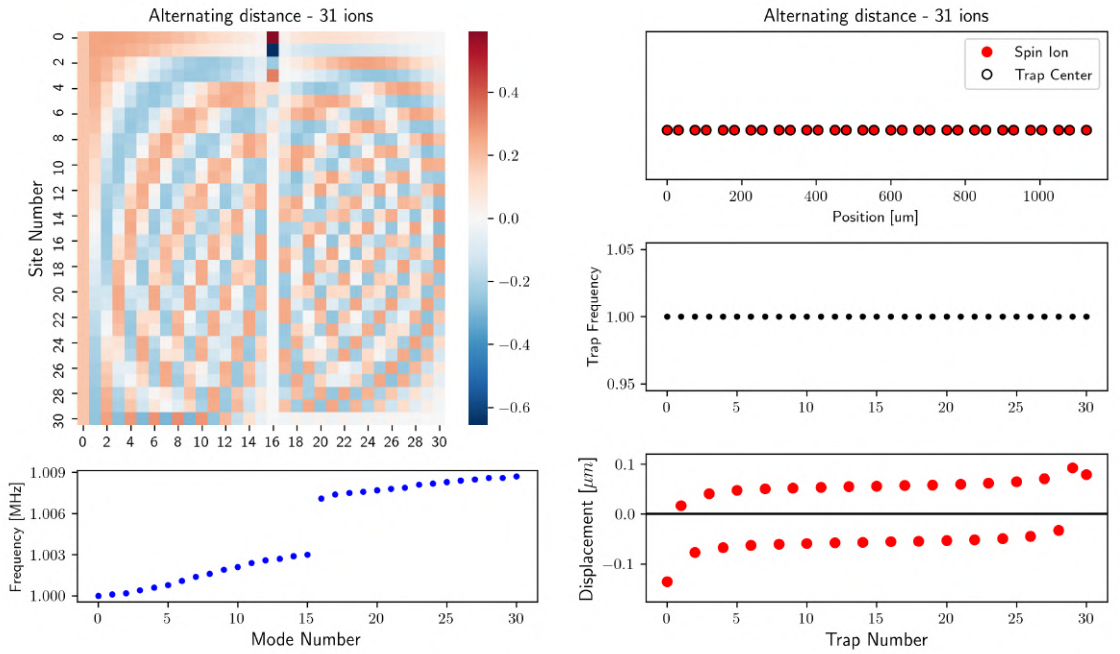

Figure 7: Simulation of a chain of 31 ions with with $m = 40$ amu, $\nu_i = 1$ MHz, and alternating distances $d_1 = 30$ μm and $d_2 = 45$ μm. The second figure shows the arrangement of the ions ad well as frequencies of microtraps and equilibrium positions of ions.

The comparison of the simulation to the results from equation (60) can be seen in figure (8). In this case, the analytical results don't agree with the simulation results, as before the frequencies are lowered due to limiting ourselves to only nearest neighbor interactions. There is also a mode with eigenfrequency set precisely halfway between the two sets of modes ($\lambda_0 = \beta$), which does not appear in the simulated results. As for the eigenvectors, while the same mode structure is present in the simulation from figure (7), the localized mode in the analytical result is localized in the last ion, while in the simulation it is in the first one of the chain.

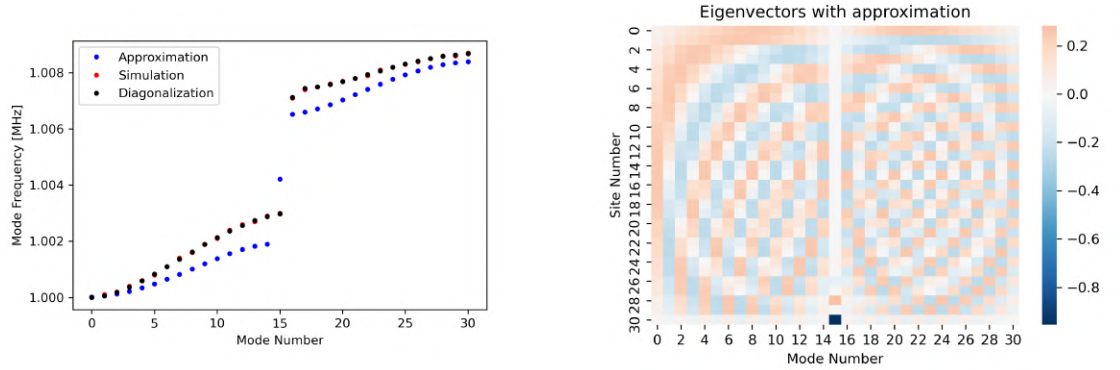

Figure 8: Left figure shows the comparison between the eigenvalues in equation (60) and the simulation with 31 ions, alongside a diagonalization of the matrix defined by (22). Right figure plots the eigenvectors resulting from the numerical diagonalization of the matrix (55).

The disparity present in figure (8) can be explained by the equilibrium positions in figure (7). The first ion in the simulation is almost twice as far form the second ion compared to any two ions in the group chain, breaking the symmetry of the system. To fix the ion equilibrium positions we

introduced two ions on each side with microtrap frequencies of $\nu = 100$ MHz such that they are decoupled from the modes of the chain with 31 ions as seen in figure (9).

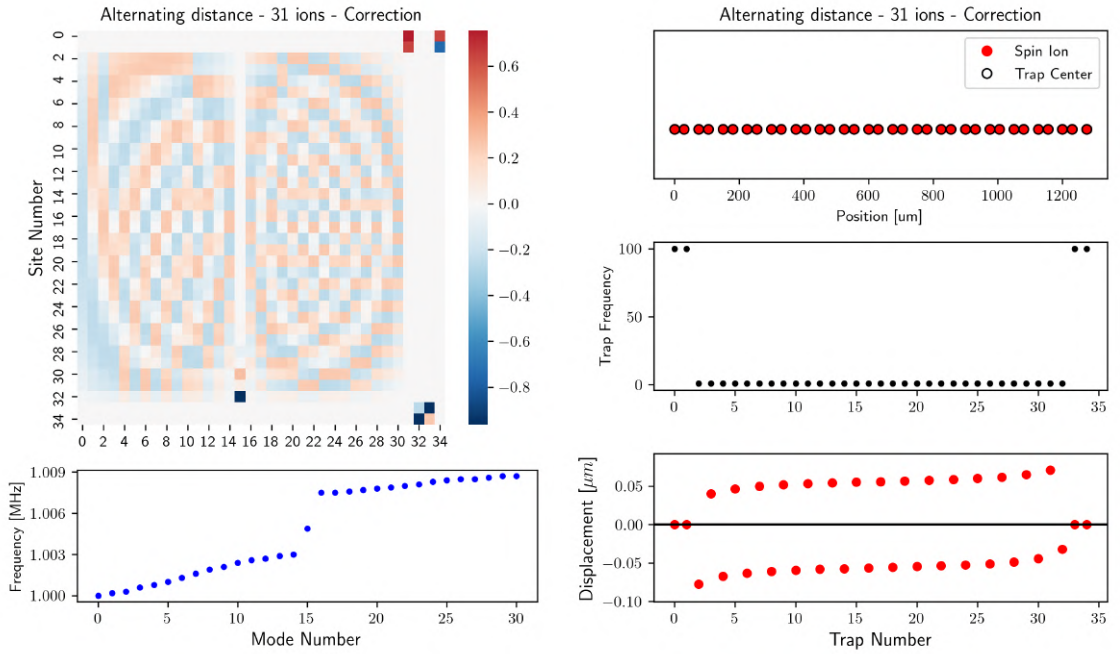

Figure 9: Simulation of a chain of 35 ions with with $m = 40$ amu, and alternating distances $d_1 = 30$ μm and $d_2 = 45$ μm. The frequency of the first two and last two microtraps is $\nu = 100$ while for the rest is $\nu = 1$. The second figure shows the arrangement of the ions ad well as frequencies of microtraps and equilibrium positions of ions.

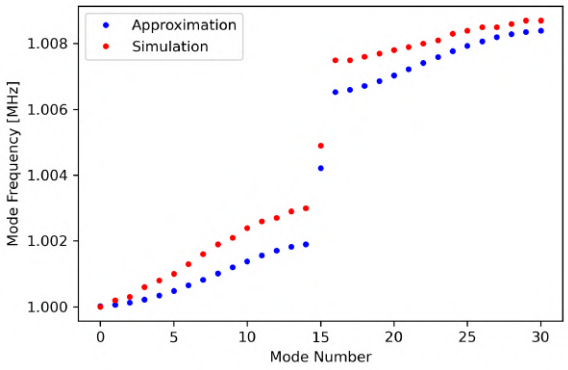

Figure 10: Comparison between the eigenvalues in equation (60) and simulations with 35 ions with high frequency traps in the edges to correct the equilibrium positions.

From the frequency comparison in figure (10), and the mode structure in figure (9) we can observe more similarities between the analytical and simulation results. The simulated frequencies now have the middle mode with frequency in between the first and second half, but still higher than the analytical ones. And the eigenvectors having a localized modes in the last ion rather than the first one. Similar findings were found for the case of an even number of ions, where edge traps with high frequencies were required to have the structure similar to the matrix (55).

The results in this section highlight the advantage of developing analytical models in parallel with numerical ones. With the former ones giving us insight into what else can be achieved by the later ones. In this case predicted the existence of localized modes in the edges with distinct frequency from the rest of the other modes.

3.3 Periodic Boundary Conditions

In this section we will consider the more exotic case of periodic boundary conditions. Where the coupling from the first ion and the last ion is the same as the first to the second one. As opposed to the previous two cases, this model is exactly solvable, with the caveat of of not being physically implementable in a one dimensional case. Although in the case of two dimensions we will see that it's possible to recreate the some of these results.

When writing down the contribution, the hessian matrix takes the form of a circulant symmetric matrix where each of the subsequent columns is a permutation of the previous one:

$$A = \begin{pmatrix} \beta & g_1 & \cdots & g_2 & g_1 \\ g_1 & \beta & \cdots & g_3 & g_2 \\ g_2 & g_1 & \cdots & g_4 & g_3 \\ \vdots & \vdots & \ddots & \vdots & \vdots \\ g_{\frac{N}{2}-1} & g_{\frac{N}{2}-2} & \cdots & g_{\frac{N}{2}+1} & g_{\frac{N}{2}} \\ g_{\frac{N}{2}} & g_{\frac{N}{2}-1} & \cdots & g_{\frac{N}{2}+2} & g_{\frac{N}{2}+1} \\ g_{\frac{N}{2}+1} & g_{\frac{N}{2}} & \cdots & g_{\frac{N}{2}+3} & g_{\frac{N}{2}+2} \\ \vdots & \vdots & \ddots & \vdots & \vdots \\ g_3 & g_4 & \cdots & g_1 & g_2 \\ g_2 & g_3 & \cdots & \beta & g1 \\ g1 & g_2 & \cdots & g_1 & \beta \end{pmatrix} \tag{61}$$

For a size N even. In the case of N odd the maximum index would be $g_{(N-1)/2}$. The values of the variables are in this case not as straight forward as before, with β taking different values depending on whether N is even or odd:

$$\beta = 1 + \frac{4l^3}{d^3} \sum_{j=1}^{\lfloor \frac{N-1}{2} \rfloor} \frac{1}{j^3} \quad if \;\; N\, odd \tag{62}$$

$$\beta = 1 + \frac{4l^3}{d^3} \left(\sum_{j=1}^{\lfloor \frac{N-1}{2} \rfloor} \frac{1}{j^3} + \frac{4}{N^3} \right) \quad if \;\; N\, even \tag{63}$$

$$g_i = -\frac{2l^3}{d^3} \frac{1}{i^3} \tag{64}$$

The eigenvalues and eigenvectors of this matrix are obtained by expressing the matrix (61) as a linear combination of a permutation matrix, which is itself diagonalizable by the discrete Fourier transform [14]. They take the form:

$$q_i^{(j)} = \rho_k^i \qquad \lambda_j = \beta + g_1\rho_j + g_2\rho_j^2 + \cdots + g_1\rho_j^{N-1} \tag{65}$$

with $q_i^{(j)}$ being the ith component of the jth eigenvector, λ_j the jth eigenvalue, and $\rho_j = e^{i2\pi j/N}$. In our case, the matrix is symmetric, so the eigenvalues will be real and can be expressed more concisely as:

$$\lambda_i = \beta + 2\sum_{j=1}^{\lfloor\frac{N-1}{2}\rfloor} g_j \cos\left(\frac{2\pi ij}{N}\right) \quad N\ odd \tag{66}$$

$$\lambda_i = \beta + 2\sum_{j=1}^{\lfloor\frac{N-1}{2}\rfloor} g_j \cos\left(\frac{2\pi ij}{N}\right) + g_{\frac{N}{2}}(-1)^i \quad N\ even \tag{67}$$

An important observation that can be made is that of the degeneracy $\lambda_i = \lambda_{N-i}$, expect in the case λ_0 where it will be the sum of the values of a column in the matrix. In the case when N is even the eigenvalue $\lambda_{N/2} = \beta + \sum_{j=0}^{N/2} g_j(-1)^j$ will also not be degenerate.

Substituting the values of the variables into the expressions:

$$\lambda_i = 1 + \frac{8l^3}{d^3}\sum_{j=1}^{\lfloor\frac{N-1}{2}\rfloor} \frac{1}{j^3}\sin^2\left(\frac{\pi ij}{N}\right) \quad N\ odd \tag{68}$$

$$\lambda_i = 1 + \frac{8l^3}{d^3}\left[\sum_{j=1}^{\lfloor\frac{N-1}{2}\rfloor} \frac{1}{j^3}\sin^2\left(\frac{\pi ij}{N}\right) + \frac{4}{N^3}\delta_{i\ mod(2),1}\right] \quad N\ even \tag{69}$$

$$\tag{70}$$

For the eigenvectors, the degeneracy in the pairs $(j, N-j)$ allows us to write linear combinations such that the resulting pair has real components:

$$\mathbf{b}_i^{(j)} = \frac{1}{2}(\mathbf{q}_i^{(j)} + \mathbf{q}_i^{(N-j)}) = \frac{1}{\sqrt{N}}\cos\left(\frac{2\pi jk}{N}\right) \tag{71}$$

$$\mathbf{b}_i^{(N-j)} = \frac{1}{2i}(\mathbf{q}_i^{(j)} - \mathbf{q}_i^{(N-j)}) = \frac{1}{\sqrt{N}}\sin\left(\frac{2\pi jk}{N}\right) \tag{72}$$

Although it's possible to express them in this simple form, the degeneracy means there is not a unique description for them. So the numerical eigenvectors are not necessarily just sines and cosines as can be seen from the figures (11) and (12).

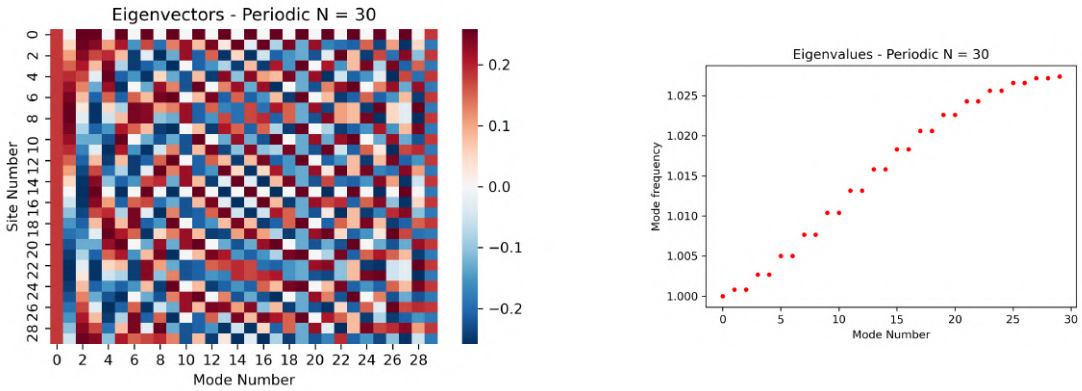

Figure 11: Eigenvalues and eigenvectors of a periodic array with N = 30 and a distance of 30 micrometers apart

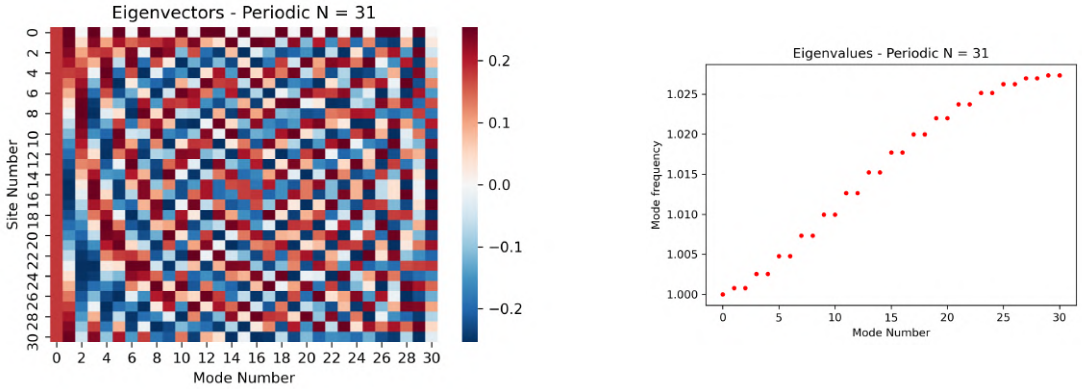

Figure 12: Eigenvalues and eigenvectors of a periodic array with N = 31 and a distance of 30 micrometers apart

4 Localized modes in microtrap arrays

One of the objectives of this work is to find combinations of parameters that would result in motional modes that have desirable contributions from different ions in the chain. A good example would be the result from [12] replicated in figure (13), where the interaction is localized on three modes, with each ion interacting weakly with other two. This is done mainly by the mechanism outlined in section 2.2.1, where different frequency microtraps tend to not interact if tuned beyond a certain threshold amount.

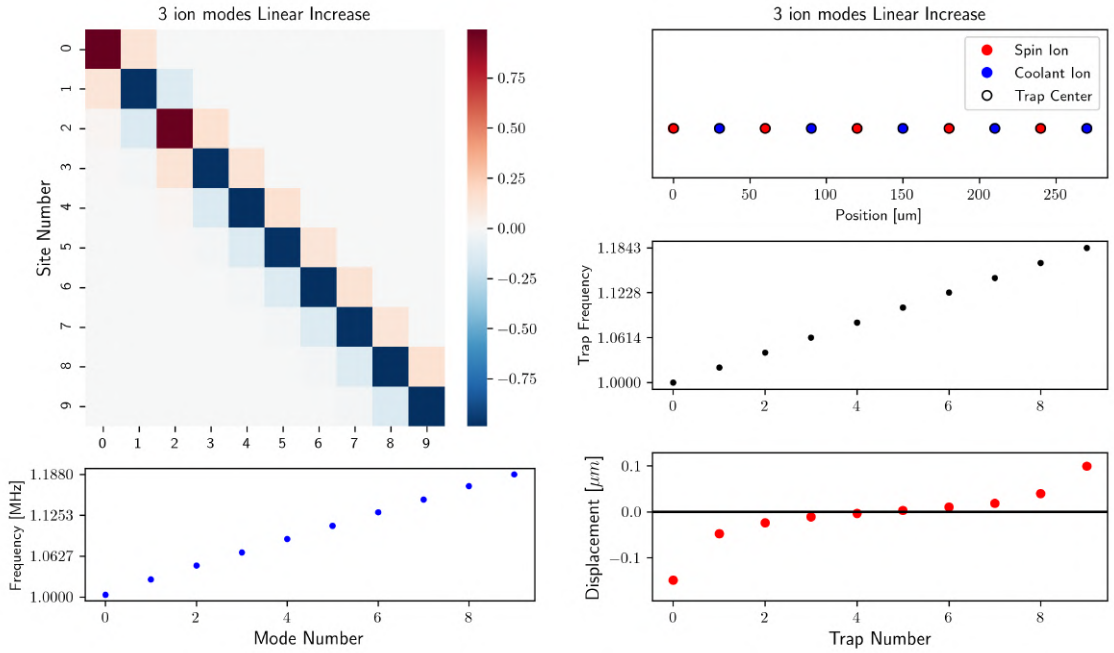

Figure 13: Simulation of a chain of 10 ions with linear frequency increases of 33 kHz for the microtraps. With alternating masses of 40 amu for coolant and 43 amu for spin ions and a distance of $d = 30$ μm

The current goal is to have a system composed of two species, one acting as a coolant ($^{40}Ca^{+}$ with m = 40 amu) and another one as a spin ion ($^{43}Ca^{+}$ with m = 43 amu), with modes where 3 spin ions are interacting with each other an there is at least one coolant ion. One way of archiving this is by using the same strategy as before of linearly increasing the frequency of the microtraps but by a smaller amount. The mode structure of such configuration can be seen in figure (14)

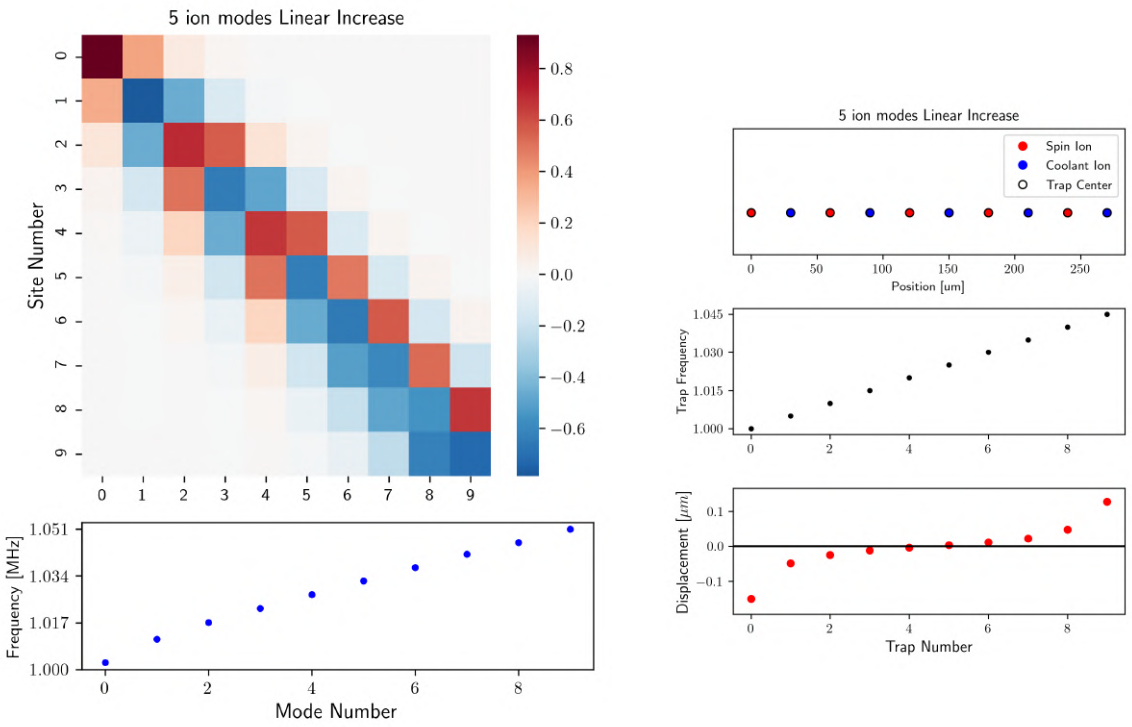

Figure 14: Simulation of a chain of 10 ions with linear frequency increases of 5 kHz for the microtraps. With alternating masses of 40 amu for coolant and 43 amu for spin ions and a distance of $d = 30$ μm between microtraps

The problem with this configuration is that each spin ion has contributions in five different modes. This is because, asides from the three modes where there are three spin ion, there are two modes where there is a majority of coolant ions and only two spin ions. In theory we could simply not address those modes and work with the ones we like, but with only around 10 kHz of difference between the desired and undesired modes, this could probe to be difficult.

As a workaround for this problem we propose a different frequency configuration. In the case above each coolant ion participates in three modes with three coolant and two spin ions, and two modes with two coolant and three spin ions, mirroring the spin ions. Such that if we would wish to select only the desirable modes, each spin ion would participate in three modes and each coolant ion in two modes. As an additional restriction, its clear the need of an increasing frequency for the spin microtraps, otherwise there would be no mode localization and the structure would be similar to the ion string we presented before.

To proceed, the coolant ions were given a higher frequency than the spin ions, not too much as to completely decouple them from the chain, but also enough such that it weakly interacts with its neighboring spin ions. So in theory only only those two modes would interact with the spin ions, as desired, and the rest of the interacts with the other coolant ions would be separated by a frequency of around 50 kHz from the modes in the spin chain. As for the spin ions we implemented the same linear increase as before, such that they only interact with their nearest neighbor spin ions. Figure (15) shows a simulation with these constrains

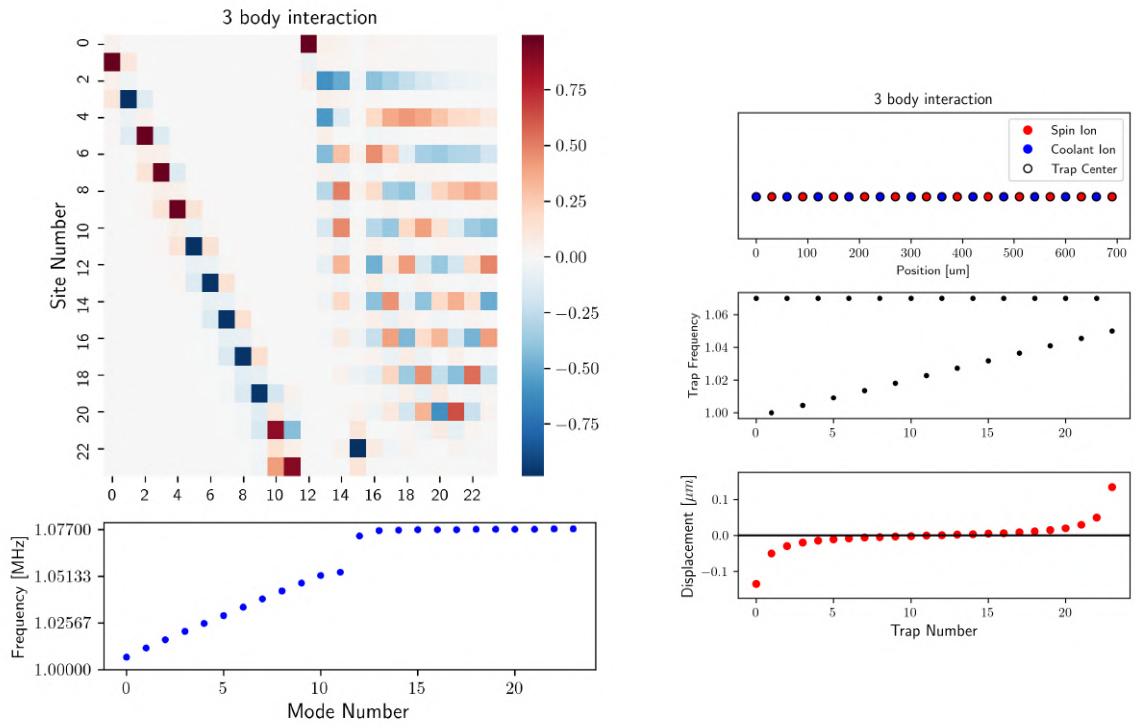

Figure 15: Simulation of a chain of 24 ions with the coolant ions having a constant frequency of 1.07 MHz and spin ions linearly increasing their frequency by 5 kHz.

There are some obvious disadvantages with these approach, mainly the interaction of the spin ions with the coolant ions is particularly weak. Also, the number of ions in a chain possible is limited by how much you can separate the frequency of the coolant ions without isolating them from the spin ions, which limits how many spin ions can be put with increasing frequency until you reach the frequency of the coolant ions. Its not possible to fix this by also increasing the frequency of the coolant ions, because this would create and asymmetry where they don't interact with the same strength between the neighboring spin ions. Still, this is just an example of the flexibility of using individually tunable microtrap arrays to perform normal mode engineering.

5 2D structures

Using the same simulation strategy as the 1D case, its possible to create arrays of potentials in a 2D plane. This idea was explored with Micro-Penning traps in [5], but here we assume independent harmonic trapping potentials, such that we can increase the trapping frequency in the z direction without affecting the modes in the x-y plane. The mode structure becomes more complicated as well, with mixing of the x and y coordinates, then each ion not only has an amplitude related to its motion, but a direction as well. With the additional coordinate there is also a total of 2N modes of motion in the system. For the simulations that are presented below the x-y microtrap potentials were circularly symmetric, meaning $\omega_x = \omega_y$, but with only a parameter change as an input, it is possible to modify the shape of these potentials to generate ellipses in any desirable direction.

In figure (16) we can observe the mode structure of a hexagon. An interesting feature being the high number of modes with degeneracy that are present, likely due to the high rotational symmetry of the system.

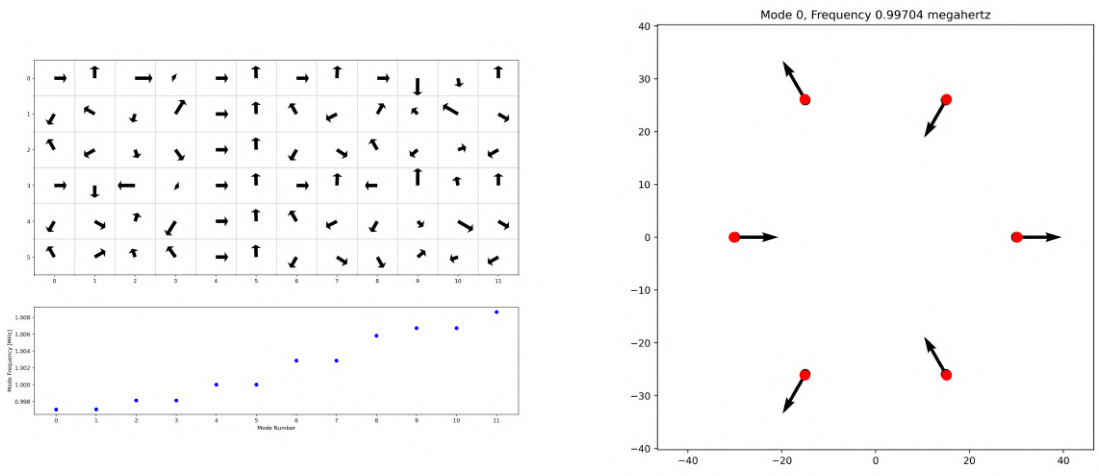

Figure 16: Hexagonal array of ions with a radius of $r = 30\mu m$ and ions with $m = 40$ amu

The additional complexity of 2D arrays can have its benefits, for its possible to construct the periodic arrays we did the calculations for in the previous section. In the case of a big circle of ions in the 2D plane, plotting the mode structure projected onto the x and y axis respectively as we can see in figure (17), greatly resembles the mode structure seen in figures (11) and (12). The differences arise from the angle dependent contribution of each ion. For example, the two ions that are horizontally separated in the x-axis have no y-coordinate interaction, while the ions precisely next to them have almost none x-coordinate force either. Although not done in this work, I believe it's possible to use the periodic boundary condition approach to find the analytical solutions for the circular system.

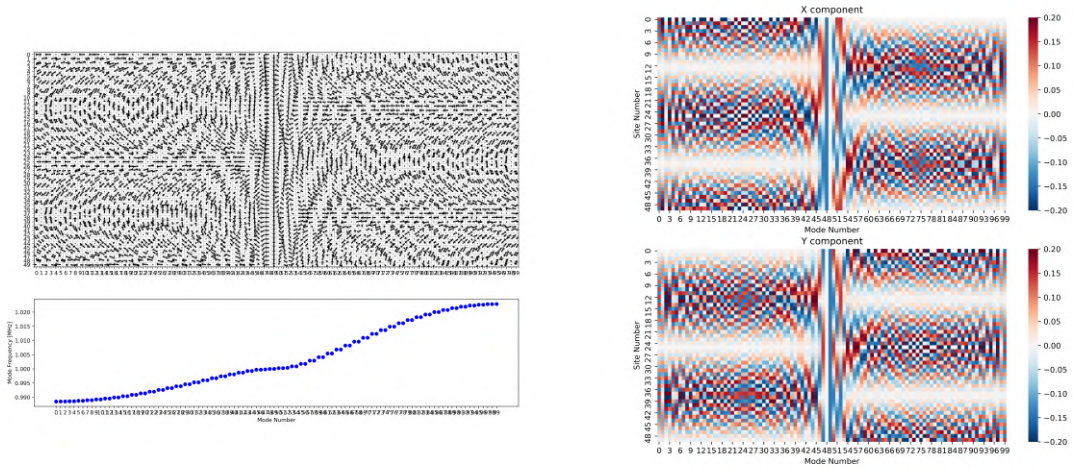

Figure 17: Vector mode structure for an array of 150 ions arranges in a circle of radius of $r = 350\mu$ m and ions with $m = 40$ amu

To further showcase the robustness of the simulation package we present in figure (18) other examples of modes in 2D arrays, one being a 5x5 grid and another an extended hexagonal array. The highly circular symmetry of both systems highly encourages analysis of the mode structure to be decomposed in a coordinate system that rotates with the systems but that is beyond the scope of this work.

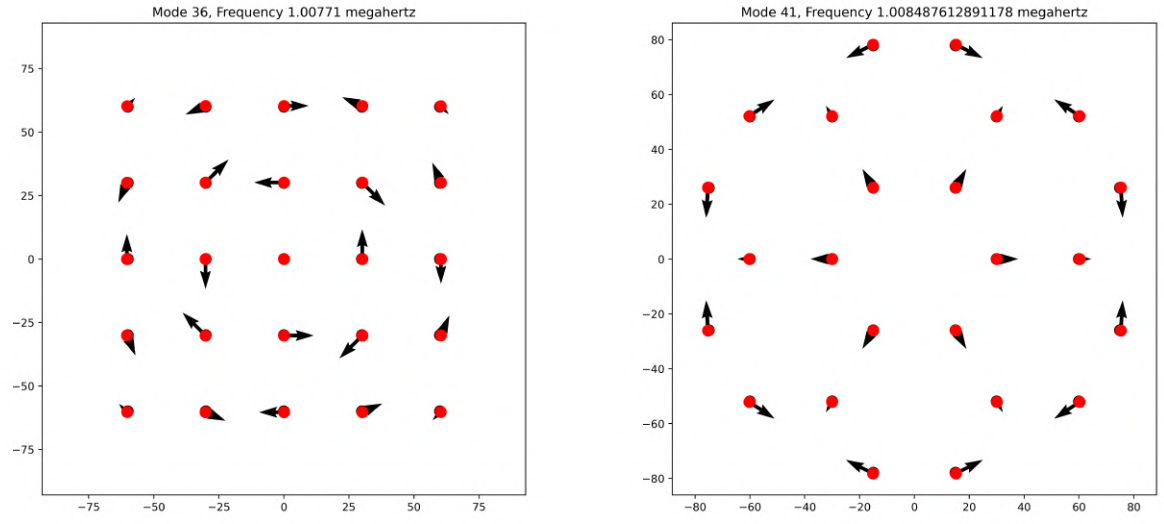

Figure 18: Example of motional modes for a 5x5 grid array (left) and hexagonal array (right) with m = 40 amu

6 Conclusion

In this work, we reviewed the treatment of motional modes for ions in a harmonic potential, to further expand it into the case of arbitrarily spaced microtraps with each one having individually tuned frequencies. Focusing on the case of only one ion per trap, we derived the equivalent equations to determine the frequency and structure of the motional modes of the array, as well as comparing these results with numerical simulations in python to test their validity.

With analytical and numerical tools we explored the solutions and structures of motional normal modes and their frequencies, using approximations such as only considering nearest-neighbor interactions to find approximate solutions to some configurations. By solving the simplified analytical problems we were able to identify particular characteristics that weren't immediately evident from the numerical solutions, such as the frequency splitting in the case of alternating distances or the mode degeneracy present in the periodic boundary condition. Although most of the microtrap configurations were only studied numerically, we obtained a good qualitative knowledge of their mode structure such as expecting ions to only weakly interact in case of detuned microtrap frequencies, a sinusoidal type modes for long chains. We even extended our simulation results for 2D arrays, but did not study them as extensively as in the 1D case.

With this knowledge of mode structures, it is possible to construct arrays that localize interactions to only a selected number of ions. This is done mainly through linearly increasing the frequency by a certain amount. While previously this was limited to 3 modes we proposed a structure where interactions with groups of 5 ions per mode but with specific ions only participating in 3 of these

modes. This is only a preliminary result so it can be further tuned, but it shows potential for the construction of more complex more structures with localized modes.

This is just an exploratory work on the richness of the motional mode structures of microtrap arrays, so there is still lots of work to be done to fully understand what is possible to archive. The complexity of the system even in 1D shows great promise for what can be done with these systems, and we hope that this discussion and tools develop here serves only as starting point for future work and applications in microtrap arrays.

References

[1] J I Cirac and P Zoller. A scalable quantum computer with ions in an array of microtraps. *Nature*, 404:579–581, 2000.

[2] Zohreh Davoudi, Norbert M Linke, and Guido Pagano. Toward simulating quantum field theories with controlled phonon-ion dynamics: A hybrid analog-digital approach. (2):1–26, 2021.

[3] M. J.C. Gover. The eigenproblem of a tridiagonal 2-Toeplitz matrix. *Linear Algebra and Its Applications*, 197-198(C):63–78, 1994.

[4] J. P. Home, D. Hanneke, J. D. Jost, D. Leibfried, and D. J. Wineland. Normal modes of trapped ions in the presence of anharmonic trap potentials. *New Journal of Physics*, 13, 2011.

[5] S. Jain, J. Alonso, M. Grau, and J. P. Home. Scalable Arrays of Micro-Penning Traps for Quantum Computing and Simulation. *Physical Review X*, 10(3):31027, 2020.

[6] D. F.V. James. Quantum dynamics of cold trapped ions with application to quantum computation. *Applied Physics B: Lasers and Optics*, 66(2):181–190, 1998.

[7] Michael Johanning. Isospaced linear ion strings. *Applied Physics B: Lasers and Optics*, 122(4):1–17, 2016.

[8] D. Maclaurin, D. Duvenaud, M. Johnson, and J. Townsend. Autograd. `https://github.com/HIPS/autograd`, 2015.

[9] Manuel Mielenz, Henning Kalis, Matthias Wittemer, Frederick Hakelberg, Ulrich Warring, Roman Schmied, Matthew Blain, Peter Maunz, David L Moehring, Dietrich Leibfried, and Tobias Schaetz. Arrays of individually controlled ions suitable for two-dimensional quantum simulations. *Nature Communications*, 7(May), 2016.

[10] Silvia Noschese, Lionello Pasquini, and Lothar Reichel. Tridiagonal toeplitz matrices: properties and novel applications. *Numerical Linear Algebra with Applications*, 20(2):302–326, 2013.

[11] J. M. Pino, J. M. Dreiling, C. Figgatt, J. P. Gaebler, S. A. Moses, M. S. Allman, C. H. Baldwin, M. Foss-Feig, D. Hayes, K. Mayer, C. Ryan-Anderson, and B. Neyenhuis. Demonstration of the trapped-ion quantum CCD computer architecture. *Nature*, 592(7853):209–213, 2021.

[12] Florentin Reiter, Florian Lange, and Zala Lenarcic. Engineering generalized Gibbs ensembles with trapped ions. *arXiv*, pages 1–17, 2019.

[13] Anders Sørensen and Klaus Mølmer. Quantum computation with ions in thermal motion. *Physical Review Letters*, 82(9):1971–1974, 1999.

[14] Garry J Tee. Eigenvectors of block circulant and alternating circulant matrices. *Res. Lett. Inf. Math. Sci.*, 8:123–142, 2005.

[15] A C Wilson, Y Colombe, K R Brown, E Knill, D Leibfried, and D J Wineland. Tunable spin-spin interactions and entanglement of ions in separate potential wells. *Nature*, 512, 2014.

[16] D. J. Wineland, C. Monroe, W. M. Itano, D. Leibfried, B. E. King, and D. M. Meekhof. Experimental Issues in Coherent Quantum-State Manipulation of Trapped Atomic Ions. *Journal of Research of the National Institute of Standards and Technology*, 103(3):259–328, 1998.

[17] K. Wright, K. M. Beck, S. Debnath, J. M. Amini, Y. Nam, N. Grzesiak, J. S. Chen, N. C. Pisenti, M. Chmielewski, C. Collins, K. M. Hudek, J. Mizrahi, J. D. Wong-Campos, S. Allen, J. Apisdorf, P. Solomon, M. Williams, A. M. Ducore, A. Blinov, S. M. Kreikemeier, V. Chaplin, M. Keesan, C. Monroe, and J. Kim. Benchmarking an 11-qubit quantum computer. *Nature Communications*, 10(1):1–6, 2019.

[18] Dayou Yang, Gouri Shankar Giri, Michael Johanning, Christof Wunderlich, Peter Zoller, and Philipp Hauke. Analog quantum simulation of (1+1) -dimensional lattice QED with trapped ions. *Physical Review A*, 94(5):1–19, 2016.

Eidgenössische Technische Hochschule Zürich
Swiss Federal Institute of Technology Zurich

Declaration of originality

The signed declaration of originality is a component of every semester paper, Bachelor's thesis, Master's thesis and any other degree paper undertaken during the course of studies, including the respective electronic versions.

Lecturers may also require a declaration of originality for other written papers compiled for their courses.

I hereby confirm that I am the sole author of the written work here enclosed and that I have compiled it in my own words. Parts excepted are corrections of form and content by the supervisor.

Title of work (in block letters):

LOCALIZED MODES IN MICROTRAP ARRAYS

Authored by (in block letters):

For papers written by groups the names of all authors are required.

Name(s):	**First name(s):**
Nuya Hernandez	Javier

With my signature I confirm that

- I have committed none of the forms of plagiarism described in the 'Citation etiquette' information sheet.
- I have documented all methods, data and processes truthfully.
- I have not manipulated any data.
- I have mentioned all persons who were significant facilitators of the work.

I am aware that the work may be screened electronically for plagiarism.

Place, date

15/09/2021

Signature(s)

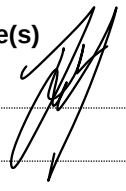

For papers written by groups the names of all authors are required. Their signatures collectively guarantee the entire content of the written paper.